Geometry-Based Approach to Find the Egg-Shape Parameters

Aysylu Gabdulkhakova[1(✉)] and Walter G. Kropatsch[2]

[1] Sirius University of Science and Technology, Sirius, Russia
aysylu@prip.tuwien.ac.at
[2] Vienna University of Technology, Vienna, Austria
krw@prip.tuwien.ac.at

Abstract. The present paper makes the next step in understanding the geometric properties of the egg-shape. It expands the possibilities of shape representation in computer vision applications. The noniterative linear algorithm finds the egg-shape given only a few parameters of the binary object: the locations and radii of the smallest enclosing circle and largest inscribed circle. This work addresses a problem of efficiently expressing a higher-order curve of a particular nature. Therefore, the experimental setup considered synthetic data of the perfect egg-shape.

Keywords: egg-shape · multifocal ellipse

1 Introduction

Efficient shape representation is one of the fundamental tasks in computer vision applications [9]. The classical approach is to approximate a complex shape with a geometric primitive such as an ellipse [3]. On one side, it provides a description of the particular characteristics: area, elongation, orientation. On the other side, it is computationally less expensive to store five parameters defining the ellipse, than to keep all the contour points of the shape in memory [4]. An egg-shape has an additional parameter - a positive weight at one of the focal points. It enables to express a wider variety of real-world objects, that resemble an oval rather than a perfect ellipse [9]. When studying the deformation of nonrigid elliptic objects, like cells, the egg-shape could express the observed change quantitatively.

This paper presents the discovered geometric properties of the egg-shape from the perspective of its smallest enclosing circle (SEC) and image processing algorithms. The idea rests on the fact that any generalized conic degenerates into a circle at infinity [4]. The derived exact relations are used to create a noniterative linear approach for computing the egg-shape parameters.

The remainder of the paper is organized as follows. Section 2 overviews the terminology related to the ellipse, the egg-shape, and SEC. Section 3 discusses the circularity, as a classical image processing way of measuring the deviation of a shape from a circle. Section 4 explains the discovered geometric properties, which

© The Author(s), under exclusive license to Springer Nature Switzerland AG 2027
M. De Marsico et al. (Eds.): ICPR 2026, LNCS 16818, pp. 79–95, 2027.
https://doi.org/10.1007/978-3-032-31397-3_6

are later used in Sect. 5 as a vital part of the proposed algorithm. Section 6 is dedicated to the comparison with the state-of-the-art work (Hladůvka et al. [9]). Section 7 concludes the paper.

2 Terminology

To simplify the explanation, let $\mathsf{d}(P_1, P_2)$ denote the Euclidean distance between the pair of points $P_1 = (x_1, y_1)$ and $P_2 = (x_2, y_2)$.

Definition 1 (Ellipse). *An ellipse, $\mathsf{E}(F_1, F_2; a)$, is the locus of points that have a constant sum of the distances to the focal points (F_1 and F_2). This sum equals $2a$ and expresses the major axis length or the length of a line segment connecting the farthest points of the ellipse:*

$$\mathsf{E}(F_1, F_2; a) = \{P \in \mathsf{R}^2 : \mathsf{d}(P, F_1) + \mathsf{d}(P, F_2) = 2a\} \tag{1}$$

The ellipse can be generalized into a higher-order curve by introducing a positive weight $\mu \in (0, 1]$ to one of its focal points [4].

Definition 2 (Egg-shape). *Consider two focal points F_1 and F_2 with positive weights $w_1 = 1, w_2 = \mu$, where $\mu \in (0, 1]$. The egg-shape, $\mathsf{ES}(F_1, F_2, \mu; c)$, is the locus of points with a constant weighted sum of the distances to the foci ($2c$):*

$$\mathsf{ES}(F_1, F_2, \mu; c) = \{P \in \mathsf{R}^2 : \mathsf{d}(P, F_1) + \mu\mathsf{d}(P, F_2) = 2c\} \tag{2}$$

The *major axis* of the egg-shape is the line segment connecting its farthest points along the line containing F_1 and F_2. Some examples are demonstrated in Fig. 4. In particular, the solid curve shows the upper half of the egg-shape with the foci F_1 and F_2.

The existing literature proposes alternative names related to the above curves: multifocal ellipse [4,6], generalized conic [4,8], polyconic [11], multifocal curve [6], polyellipse [11], n-ellipse [13], k-ellipse [12], oval [10], and Cartesian oval [15].

Prior to further discussion, let us agree on the egg-shape major axis to be aligned with the x-axis and on the origin to be at F_1. So, the foci coordinates are: $F_1 = (0, 0)$, $F_2 = (2f, 0)$. Table 1 summarizes the notations used throughout the paper. In particular, the usage of m and n enables simplification of (2):

$$\mathsf{ES}(F_1, F_2, \mu; c) = \{P \in \mathsf{R}^2 : m + \mu n = 2c\} \tag{3}$$

Proposition 1 (Convexity) *The egg-shape is convex [4].*

Proposition 2 (Compactness) *The egg-shape is compact [4].*

Proposition 3 (Symmetry) *The egg-shape is symmetric about its major axis.*

Proof Let us reformulate (2) for any egg-shape point $P = (x, y)$ by explicitly using the Euclidean distance in 2D:

$$\mathcal{F}(x, y) = \sqrt{x^2 + y^2} + \mu\sqrt{(x - 2f)^2 + y^2} - 2c \tag{4}$$

As can be noticed, the sign of y-coordinate does not affect the result of (4), which is not the case for x-coordinate.

Proposition 4. *SEC of a convex set is unique [14].*

Table 1. Egg-shape parameters.

Symbol	Description	Symbol	Description
$F_1 = (0, 0)$ $F_2 = (2f, 0)$	Focal points	$2f$	Focal length, $\mathtt{d}(F_1, F_2)$
μ	Weight of F_2, $\mu \in (0, 1]$. Cosine of the sharp corner half-angle [4]	$2c$	Weighted sum of the distances to F_1 and F_2
A, B	Endpoints of the major axis	$2R$	Major axis length, $\mathtt{d}(A, B)$; SEC diameter
m	Distance from the egg-shape point to F_1	n	Distance from the egg-shape point to F_2
$K = (t, r)$	y-axis extremum of the upper half of the egg-shape	$K' = (t, 0)$	Projection of K onto $\overline{F_1F_2}$
α	$\angle K'KF_1$	β	$\angle K'KF_2$
ψ	$\frac{\beta-\alpha}{2}$	ϕ	$\angle K'KO$
τ	$\cos(\beta - \alpha)$	O	SEC centre
k	Distance between O and K'	r	Distance between K and K'

3 Circularity of the Shape

In digital image processing [7] there is a measure describing an arbitrary shape by its similarity to the circle. It is called roundness (or circularity). The roundness is computed as the following ratio: $\frac{4\pi A}{p^2}$, where A denotes the area of the 2D shape, and p corresponds to its perimeter.

In the case of elliptic shapes, the deviation from the circle could be expressed by eccentricity [7]. Formally, the eccentricity equals: $\varepsilon(a, b) = \frac{\sqrt{a^2-b^2}}{a}$, where a and b denote the lengths of the semi-major and semi-minor axes accordingly.

In the case of egg-shapes, the ellipse eccentricity does not reflect the impact of weights at the foci. Hladůvka et al. [9] redefine this measure to depend on two parameters: the smallest weight among the pair of foci ($0 < \mu \leq 1$) and the multiplier (c) applied to the focal distance: $\varepsilon(c, \mu) \approx \frac{1}{c}\ \mu^{S(c)}$, where $S(c)$ encompasses the observed power-law dependency between ε and μ. In contrast to this approach, the present paper studies the egg-shape not as the deviation from ellipse, but through its relation to SEC.

4 Properties of the Egg-Shape Relatively to Its SEC

The egg-shape compactness (Proposition 2) implies the existence of a circle enclosing all of its points. Due to convexity (Proposition 1), this circle is unique (Proposition 4).

Proposition 5. *Suppose the distance between two farthest egg-shape points along the major axis equals* $\mathsf{d}(A, B) = 2R$. *Then:*

$$R = \frac{2c}{1+\mu} \tag{5}$$

Proof. By Definition 2, if A and B are the endpoints of the egg-shape major axis:

$$\begin{cases} \mathsf{d}(A, F_1) + \mu\mathsf{d}(A, F_2) = 2c \\ \mathsf{d}(B, F_1) + \mu\mathsf{d}(B, F_2) = 2c \end{cases}, \tag{6}$$

At the same time, note the following equalities (Fig. 1a):

$$\begin{aligned} \mathsf{d}(A, F_2) &= \mathsf{d}(A, F_1) + 2f \\ \mathsf{d}(B, F_1) &= 2f + \mathsf{d}(B, F_2) \end{aligned}, \tag{7}$$

where $2f$ expresses the length of the line segment connecting the foci. Let us now substitute the corresponding values of $\mathsf{d}(A, F_2)$ and $\mathsf{d}(B, F_1)$ in (6) and take the sum of the resultant equations :

$$[\mathsf{d}(A, F_1) + \mathsf{d}(B, F_2) + 2f] = \frac{4c}{(1+\mu)} \tag{8}$$

The left part of the equation, $[\mathsf{d}(A, F_1) + \mathsf{d}(B, F_2) + 2f]$, in (8) equals $\mathsf{d}(A, B)$. Thus, the desired equality is achieved.

Theorem 1. *The diameter of the egg-shape SEC equals its major axis* $\overline{AB}$.

Proof. The egg-shape is a convex curve (Proposition 1). According to the properties of SEC of a convex set [1], it is unique and defined as a circle passing through either (a) two points forming its diameter or (b) three points that do not form an obtuse-angled triangle.

Earlier, (4) expressed the egg-shape using the $(x, y)-$coordinates of its points. The partial derivative of this function with respect to x equals:

$$\frac{\partial \mathcal{F}}{\partial x} = \frac{x}{\sqrt{x^2+y^2}} + \frac{\mu(x-2f)}{\sqrt{(x-2f)^2+y^2}} \tag{9}$$

Let us simplify (9) using the notations from Table 1, i.e. $m = \sqrt{x^2+y^2}$ and $n = \sqrt{(x-2f)^2+y^2}$, and group the x-parts:

$$\frac{\partial \mathcal{F}}{\partial x} = x(\frac{1}{m} + \frac{\mu}{n}) - \frac{2\mu f}{n} \tag{10}$$

By expressing n through m using (2) and substituting it in (10):

$$\frac{\partial \mathcal{F}}{\partial x} = x\left(\frac{1}{m} + \frac{\mu^2}{2c-m}\right) - \frac{2\mu^2 f}{2c-m} \tag{11}$$

The minuend in (11) is the circle with the curvature defined as $(\frac{1}{m} + \frac{\mu^2}{2c-m})$. The smaller is the curvature, the larger is the radius of the circle. Its derivative with respect to m reaches 0 at two values:

$$\mathcal{G} = \frac{1}{m} + \frac{\mu^2}{2c-m} \tag{12}$$

$$\frac{\partial \mathcal{G}}{\partial m} = \frac{m^2(1-\mu^2) - 4mc + 4c^2}{m^2(2c-m)^2} = 0 \tag{13}$$

$$m_{\pm} = \frac{2c(1 \pm \mu)}{1-\mu^2} \tag{14}$$

Since m_+ leads to negative n, the only solution corresponds to $m_- = \frac{2c}{1+\mu}$. Taking into account (5) leads to $m_- = R$ and $n = R$. Substituting these values in (10) produces:

$$\frac{\partial \mathcal{F}}{\partial x} = \frac{x}{R}(1+\mu) - \frac{2\mu f}{R} \tag{15}$$

The result is the partial derivative of the circle equation with respect to x. The radius equals R and the centre is located at $(\frac{2\mu f}{1+\mu})$. Since the origin is at F_1, the centre is the midpoint of the major axis. The circle passes through the points A and B forming the diameter which satisfies the condition of SEC.

Proposition 6. *The SEC centre, O, divides the line segment connecting the foci in the following ratio:*

$$\frac{\mathsf{d}(F_1, O)}{\mathsf{d}(O, F_2)} = \mu \tag{16}$$

Proof. Due to symmetry (Proposition 3), it is sufficient to consider only the upper half of the egg-shape (grey) and its SEC (dotted) as shown in Fig. 1a. For simplicity, the lengths of the line segments along the diameter are expressed by a single letter: $p = \mathsf{d}(A, F_1)$, $q = \mathsf{d}(F_1, O)$, $v = \mathsf{d}(O, F_2)$, $w = \mathsf{d}(F_2, B)$. According to (5), the relative point location along the diameter and (2) for B:

$$\begin{cases} R = \frac{2c}{1+\mu} \\ v + q = 2f \\ v + w = R \\ p + q = R \\ 2f + w + \mu w = 2c \end{cases} \quad (17) \quad \text{, therefore} \quad \begin{cases} p = \frac{2(c-\mu f)}{1+\mu} \\ q = \frac{2\mu f}{1+\mu} \\ v = \frac{2f}{1+\mu} \\ w = \frac{2(c-f)}{1+\mu} \end{cases} \tag{18}$$

As observed from (18), the ratio between q and v equals μ.

Proposition 7. *For y-axis extremum K of the egg-shape it is true, that:*

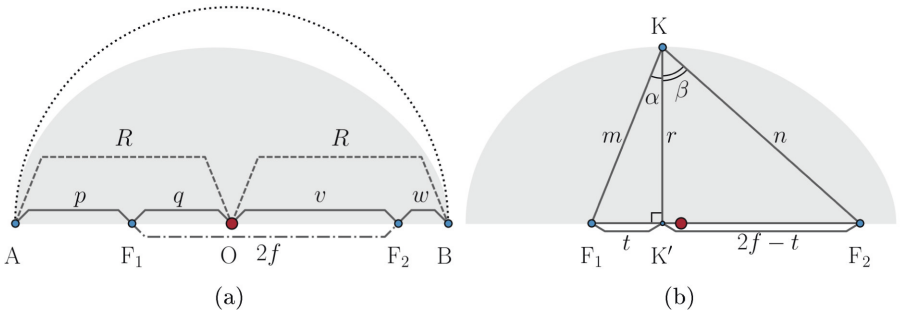


Fig. 1. The egg-shape half (grey) which major axis is aligned with x-axis. (a) SEC half (dotted line) and various line segments along its diameter (b) distances and angles related to y-axis extremum K

$$\frac{\sin\alpha}{\sin\beta} = \mu \tag{19}$$

$$\frac{\tan\alpha}{\tan\beta} = \frac{\mu m}{n} \tag{20}$$

Proof. Consider the egg-shape in Fig. 1b. For the extremum point $K(t, r)$ it is valid to assign (10) to zero, i.e. $\frac{\partial \mathcal{F}}{\partial x} = 0$, and derive the value of t and $(2f - t)$:

$$t = \frac{2\mu m f}{n + \mu m} \tag{21}$$

$$2f - t = \frac{2nf}{n + \mu m} \tag{22}$$

Then it is possible to express the desired ratios between sines and tangents:

$$\frac{\sin\alpha}{\sin\beta} = \frac{t}{m} \cdot \frac{n}{(2f - t)} = \mu \tag{23}$$

$$\frac{\tan\alpha}{\tan\beta} = \frac{t}{r} \cdot \frac{r}{(2f - t)} = \frac{\mu m}{n} \tag{24}$$

Proposition 7 conceptually complies with the Snell's law of refraction [8].

Corollary 1. *The projection of K onto $\overline{F_1F_2}$, K', is located between F_1 and O.*

Proof. Assuming the opposite, it is possible that $t > q$. Substituting (21) and (18) leads to $m > n$. Due to (19), $\cos\alpha \geq \cos\beta$. Expressing the cosines through m, n and r leads to $m \leq n$. Contradiction.

Proposition 8. *For y-axis extremum K of the egg-shape it is true, that:*

$$\tau \stackrel{def}{=} \cos(\beta - \alpha) = \frac{c \cdot \sin\beta}{f} \tag{25}$$

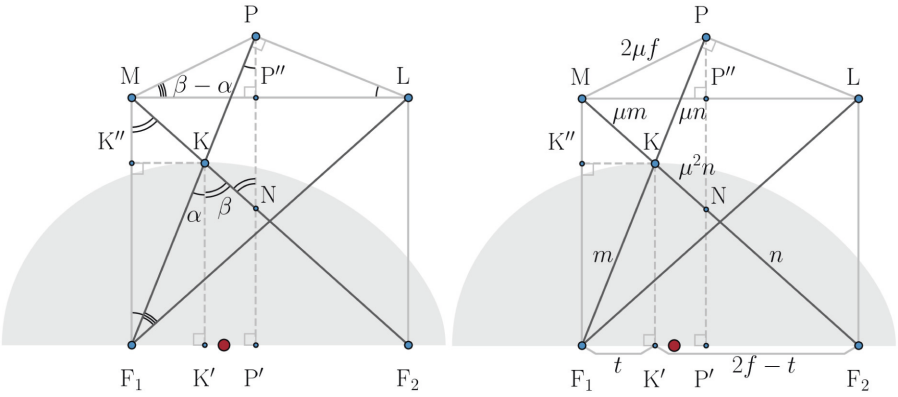


Fig. 2. (a) angles and (b) distances related to K, when extending the sides of $\triangle F_1KF_2$ by μn ($= \mathsf{d}(K, P)$), and μm ($= \mathsf{d}(K, M)$). F_1MLF_2 is a rectangle. P' and P'' are the projections of P onto $\overline{F_1F_2}$ and $\overline{ML}$. $\overline{PP'}$ intersects $\overline{MF_2}$ at N

Proof. Let the line containing $\overline{KF_2}$ and the normal to $\overline{F_1F_2}$ passing through F_1 intersect at M (Fig. 2). Then $\angle MF_1K = \alpha$ and $\angle F_1MK = \beta$ (Fig. 2a). Projecting K onto $\overline{MF_1}$ results in two right triangles, $\triangle KK''M$ and $\triangle KK''F_1$, that share the cathetus $\overline{KK''}$ of length t (Fig. 2b). Combining the sine formulas for these triangles with (19) enables to derive $\mathsf{d}(M, K)$:

$$\begin{cases} t = m\sin\alpha \\ t = \mathsf{d}(M,K)\sin\beta \\ \sin\alpha = \mu\sin\beta \end{cases} \quad (26) \quad \text{, therefore} \quad \mathsf{d}(M,K) = \mu m \tag{27}$$

Let us extend the side $\overline{F_1K}$ by μn, i.e. $\mathsf{d}(K, P) = \mu n$. The triangles $\triangle PKM$ and $\triangle F_2KF_1$ are similar [5] due to equal ratios of the side lengths and the angle between them. Thus, it is possible to find the length of $\overline{MP}$: $\mathsf{d}(M, P) = 2\mu f$.

Also it means that $\angle PMK = \frac{\pi}{2} - \alpha$ and $\angle PML = \angle PMK - \angle LMK = \beta - \alpha$. As a result, in the right triangle $\triangle PP''M$, the angle $\angle MPP'' = \frac{\pi}{2} - (\beta - \alpha)$

Let P' be the projection of P onto $\overline{F_1F_2}$. Crossing two parallel lines $\overline{KK'}$ and $\overline{PP'}$ by $\overline{F_1P}$ and $\overline{MF_2}$ leads to $\angle KPN = \alpha$, $\angle KNP = \beta$ [5]. The triangles $\triangle MKF_1$ and $\triangle NKP$ are similar and $\mathsf{d}(K, N) = \mu^2 n$. So, the length of $\overline{MN}$ equals $\mathsf{d}(M, N) = \mu(m + \mu n) = 2\mu c$. Finally, apply the sine rule [5] to $\triangle MNP$:

$$\frac{\mathsf{d}(M,P)}{\sin\beta} = \frac{\mathsf{d}(M,N)}{\sin(\frac{\pi}{2} - (\beta - \alpha))} \quad (28) \quad \text{, therefore} \quad \frac{2\mu f}{\sin\beta} = \frac{2\mu c}{\cos(\beta - \alpha)} \quad (29)$$

The desired relation is achieved by simplifying (29).

Proposition 9. *The distances from K to F_1 and F_2 can be expressed as:*

$$m = \frac{2c(\tau - \mu)}{\tau(1 - \mu^2)} \quad (30) \qquad n = \frac{2c(1 - \mu\tau)}{\tau(1 - \mu^2)} \quad (31)$$

Proof. In the right triangle $\triangle F_2F_1M$:

$$\frac{2f}{\sin\beta} = \mu m + n \quad (32)$$

The system of equations containing (32), (3) and (25) leads to the result.

Proposition 10. *The lengths t and $(2f - t)$ can be expressed as:*

$$t = \frac{2\mu f(\tau - \mu)}{(1 - \mu^2)} \quad (33) \qquad 2f - t = \frac{2f(1 - \mu\tau)}{(1 - \mu^2)} \quad (34)$$

Proof. Proved by substituting m and n from Proposition 9 to (21) and (22).

Proposition 11. *For the egg-shape, the distance between its y-axis extremum projection onto $\overline{F_1F_2}$ and its SEC centre, i.e. $k = \mathsf{d}(K', O)$, equals:*

$$k = 2f \cdot \frac{\mu(1 - \tau)}{1 - \mu^2} \quad (35)$$

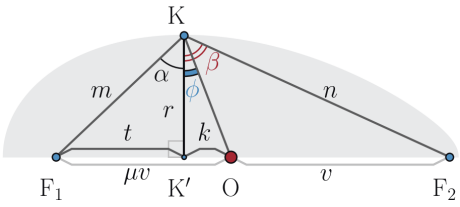


Fig. 3. Distances and angles related to K, K' and O

Proof. Consider the geometric construction in Fig. 3. Proposition 6 states the ratio between $\overline{F_1O}$ and $\overline{OF_2}$ to be μ. So, denoting $v = \mathsf{d}(O, F_2)$ implies $\mu v = \mathsf{d}(F_1, O)$.

Since $t = \mathsf{d}(F_1, K')$, then $k = \mathsf{d}(K', O) = \mu v - t$ (refer to Cor. 1). Substituting the values of v and t from (18) and (33) achieves the desired equation.

Proposition 12. *For the y-axis extremum K of the egg-shape, $\cos\alpha$ and $\cos\beta$ are related to μ and τ:*

$$\cos\alpha = \frac{1 - \mu\tau}{\sqrt{1 + \mu^2 - 2\mu\tau}} \qquad (36) \qquad\qquad \cos\beta = \frac{\tau - \mu}{\sqrt{1 + \mu^2 - 2\mu\tau}} \qquad (37)$$

Proof. Let us express the value of $\cos\alpha$ using the sine ratio in (19) and the basic relationship between sine and cosine [5]:

$$\frac{\sqrt{1 - \cos^2\alpha}}{\sqrt{1 - \cos^2\beta}} = \mu \qquad (38a)$$

$$\cos\alpha = \sqrt{1 - \mu^2 + \mu^2\cos^2\beta} \qquad (38b)$$

The right triangles $\triangle F_1K'K$, $\triangle F_2K'K$ and $\triangle OK'K$ enable to derive the ratios between the tangents of α, β and ϕ:

$$\frac{\tan\alpha}{\tan\phi} = \frac{t}{k} \qquad (39) \qquad\qquad \frac{\tan\beta}{\tan\phi} = \frac{2f - t}{k} \qquad (40)$$

After substituting t, $(2f - t)$ and k using (33), (34) and (35) respectively:

$$\frac{\tan\alpha}{\tan\phi} = \frac{\tau-\mu}{1-\tau} \quad (41) \qquad \frac{\tan\beta}{\tan\phi} = \frac{1-\mu\tau}{\mu(1-\tau)} \quad (42) \qquad \frac{\tan\beta}{\tan\alpha} = \frac{1-\mu\tau}{\mu(\tau-\mu)} \quad (43)$$

Next, it is possible to relate the cosines of α and β using the ratio between tangents (43) and sines (19):

$$\cos\alpha = \frac{\tan\beta}{\tan\alpha} \cdot \frac{\sin\alpha}{\sin\beta} \cdot \cos\beta = \frac{1-\mu\tau}{\tau-\mu} \cdot \cos\beta \quad (44)$$

Let us equate the expressions of $\cos\alpha$ from (38b) and (44):

$$\sqrt{1-\mu^2+\mu^2\cos^2\beta} = \frac{1-\mu\tau}{\tau-\mu} \cdot \cos\beta \quad (45)$$

Solving (45) for $\cos\beta$ and substituting its result in (44) finalizes the proof.

Proposition 13. *For the y-axis extremum K of the egg-shape, let $\psi \overset{def}{=} \frac{\beta-\alpha}{2}$. Then the tangents are linked as:*

$$\tan\phi = \tan\alpha \cdot \tan\beta \cdot \tan\psi \quad (46)$$

Proof. For the right triangles $\triangle F_1K'K$ and $\triangle F_2K'K$, let us express the values of m and μn using the cosine expressions from (36) and (37):

$$m = r\frac{\sqrt{1+\mu^2-2\mu\tau}}{1-\mu\tau} \quad (47) \qquad \mu n = \mu r\frac{\sqrt{1+\mu^2-2\mu\tau}}{\tau-\mu} \quad (48)$$

Substituting these results in (3) leads to:

$$r\sqrt{1+\mu^2-2\mu\tau}\frac{\tau(1-\mu^2)}{(1-\mu\tau)(\tau-\mu)} = 2c \quad (49)$$

From (38b) it is possible to derive $\sin\beta$:

$$\sin\beta = \sqrt{\frac{1-\tau^2}{1+\mu^2-2\mu\tau}} \quad (50)$$

Applying (50) and (25) to (49) produces:

$$r \cdot \frac{(1-\mu^2)\sqrt{1-\tau^2}}{(1-\mu\tau)(\tau-\mu)} = 2f \quad (51)$$

At the same time, f is associated with k by Proposition 11. Also, the multipliers and dividers can be substituted according to (41) and (42):

$$r \cdot \frac{(1-\mu^2)\sqrt{1-\tau^2}}{(1-\mu\tau)(\tau-\mu)} = k \cdot \frac{(1-\mu^2)}{\mu(1-\tau)} \tag{52a}$$

$$r \cdot \sqrt{\frac{1+\tau}{1-\tau}} = k \cdot \frac{\tan\alpha \cdot \tan\beta}{\tan^2\phi} \tag{52b}$$

Note, that $\tau \overset{\text{def}}{=} \cos(\beta-\alpha)$, so, $\sqrt{\frac{1+\tau}{1-\tau}}$ defines the half-angle tangent, i.e. $\tan\frac{\beta-\alpha}{2} = \sqrt{\frac{1-\tau}{1+\tau}}$ [5]. Also, $\tan\phi = \frac{k}{r}$. Substituting these expressions in (52b) finalizes the proof.

Proposition 14. *For the y-axis extremum K of the egg-shape holds:*

$$\mu = \frac{\Omega \pm \sqrt{\Omega^2 - 4(\tan\phi\cdot\tau)^2}}{2\tan\phi\cdot\tau}, \text{where } \Omega = \tan\phi\cdot(1+\tau^2) + \tan\psi\cdot(1-\tau^2) \tag{53}$$

Proof. Using the correspondence between sines and cosines [5] together with (36) and (37), it is possible to derive $\tan\alpha$ and $\tan\beta$:

$$\tan\alpha = \frac{\mu\sqrt{1-\tau^2}}{1-\mu\tau} \tag{54}$$

$$\tan\beta = \frac{\sqrt{1-\tau^2}}{1-\mu} \tag{55}$$

Applying (54) and (55) to (46) results in:

$$\tan\psi\cdot\mu\cdot(1-\tau^2) = \tan\phi\cdot(\tau-\mu)(1-\mu\tau) \tag{56}$$

Solving the quadratic equation (56) for μ produces the desired result.

4.1 Ranges for μ and τ

The above formulas impose limits on μ and τ. The denominators containing $(1-\mu^2)$ and $(1+\mu^2-2\mu\tau)$ turn to zero, when $\mu = 1$ (ellipse). Also $\tan\phi$ in (53) turns to zero, when the egg-shape degenerates into a circle. These situations should be treated separately.

In addition, there are limits for τ. Its maximum, $\tau = 1$, corresponds to the circle, while the minimum is related to the rightmost location of F_2. In the latter, the curve is the egg-shape with sharp corner, F_2 is on SEC and $\mathsf{d}(F_2, O) = R$. According to (18):

$$\mathsf{d}(F_2, O) = \frac{2f}{1+\mu} = R \tag{57}$$

As follows from (5) and (57), for the egg-shape with corner $c = f$. Assuming (25), it leads to $\tau \stackrel{\text{def}}{=} \cos(\beta - \alpha) = \sin\beta$. Applying the trigonometric relations [5], (19), (36) and (37) enables to express τ through μ:

$$\cos(\beta - \alpha) = \cos\beta\cos\alpha + \sin\beta\sin\alpha \tag{58a}$$

$$\tau = \frac{(1-\mu\tau)(\tau-\mu)}{1+\mu^2-2\mu\tau} + \mu\tau^2 \tag{58b}$$

$$2\tau^2 - \mu\tau - 1 = 0 \tag{58c}$$

$$\tau_{\pm} = \frac{\mu \pm \sqrt{\mu^2+8}}{4} \tag{58d}$$

Since β and α are the angles of the right triangles, their difference cannot exceed 90°. Thus, only the positive solution in (58d) is acceptable. So, given μ, the values of τ belong to $[\frac{\mu+\sqrt{\mu^2+8}}{4}, 1]$. Since $\mu \in (0, 1]$ by Definition 2, the minimum possible τ (corresponding to $\mu = 0$) equals $\frac{\sqrt{2}}{2}$. It means, for the egg-shape with both foci inside SEC the difference $(\beta - \alpha)$ is limited by the interval $[0°, 45°)$.

5 Algorithm for Finding the Egg-Shape Parameters

The paper addresses the problem of finding the egg-shape given the minimum information available from the efficient digital image processing algorithms. The difficulty of this task is the number of the required parameters to define a curve: (1)−(4) the XY coordinates of F_1 and F_2, (5) the value of the sum of the distances to the foci, (6) the foci weight. In contrast to the ellipse, the foci are not located symmetrically with respect to the origin and depend on μ (Proposition 6).

The discovered geometric relations enable reducing the original problem to the search of $(\beta - \alpha)$. Line 1 finds SEC with the classical linear-time solution [14]. Lines 2–3 estimate k and r using the linear-time Distance Transform (DT) [2]. For the binary image complement ($I^{\complement}$), it assigns the distance from every zero-pixel (shape) to the nearest nonzero pixel (background). The coordinates and values of the global maximum of the distance field relate to the centre (K') and radius (r) of the largest inscribed circle. Lines 8–11 compute the egg-shape parameters according to the equations. The desired solution minimizes the sum of the differences between the actual and computed parameters (Lines 12–14). Note the uniqueness of curves, μ and $(\beta - \alpha)$ for the same ϕ (Fig. 4).

5.1 Validity of the Error Function (Analytical)

Algorithm 1.1 fixes $\frac{k}{r}$ (Line 4) and finds for it all the possible pairs of μ and τ. Since k_e and r_e depend on μ, which, in turn, depends on $\frac{k}{r}$, their ratio is constant. The resultant absolute values of k_e and r_e form curves which derivatives change identically. Using both $|k - k_e|$ and $|r - r_e|$ enables to estimate the error at various scales. So, for the proof it is sufficient to analyse only one of the components.

According to (5), (25), (35) and (50):

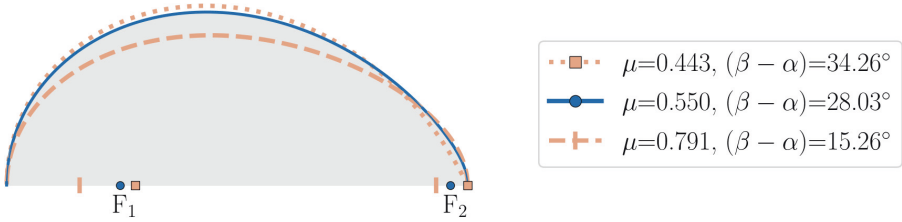


Fig. 4. The examples of egg-shape halves for the same ϕ and various $(\beta - \alpha)$. The markers show the foci locations. The groundtruth (grey area) slightly differs from the egg-shape (solid) with the foci F_1 and F_2, that has the smallest error

Algorithm 1.1: Finding the egg-shape parameters

Data: Input binary image containing the shape : I
Result: Egg-shape parameters: c, f, μ

$R, [x_R, y_R] \leftarrow$ find_SEC(I)
$r, [x_r, y_r] \leftarrow$ get_the_maximum_DT_value($I^{\complement}$)
$k \leftarrow \sqrt{(x_R - x_r)^2 + (y_R - y_r)^2}$
$\tan\phi \leftarrow \frac{k}{r}$
$c, f, \mu \leftarrow \emptyset$
$error \leftarrow \infty$
for $(\beta - \alpha) \leftarrow 0°$ **to** $45°$ *with step*=η **do**
  $\tau_e \leftarrow \cos(\beta - \alpha)$
  $\mu_e \leftarrow$ find_μ $(\beta - \alpha, \tan\phi)$ - apply (53)
  $c_e, f_e \leftarrow$ find_eggshape_parameters (μ_e, R, τ_e) - apply (5), (25)
  $r_e, k_e \leftarrow$ find_r_and_k(μ_e, c_e, τ_e) - apply (49), (35)
  if $|r - r_e| + |k - k_e| < error$ **then**
    $c, f, \mu \leftarrow c_e, f_e, \mu_e$
  end
end

$$k_e = 2f_e \cdot \frac{\mu_e(1 - \tau_e)}{1 - \mu_e^2} \qquad (59) \qquad\qquad 2f_e = R \cdot \frac{1 + \mu_e}{\tau_e} \cdot \sin\beta \qquad (60)$$

Joining them into a single equation leads to:

$$k_e = R \cdot \sin\beta \cdot \frac{\mu_e}{1 - \mu_e} \cdot \frac{1 - \tau_e}{\tau_e} \qquad (61)$$

Here, R is a constant value and does not affect the derivative. Both μ_e and τ_e denote the cosines (Tab. 1). Let us reformulate (61) with respect to these facts:

$$k_e^* = \sin\beta \cdot \frac{\cos\theta}{1 - \cos\theta} \cdot \frac{1 - \cos(\beta - \alpha)}{\cos(\beta - \alpha)} \qquad (62)$$

Generally speaking, k_e^* is a positive function. Its minimum value tends to 0. By Definition 2, $\mu \overset{\text{def}}{=} \cos\theta \in (0, 1]$, where 0 corresponds to a circle and 1 - to an ellipse or a line segment. Due to the denominator $(1 - \cos\theta)$ in (62), the latter case should be considered separately to distinguish two possible solutions. If k_e is not a monotonic function, then there must exist a critical point, where the first order partial derivatives are zero:

$$\frac{\partial k_e^*}{\partial \beta} = \left(\frac{\boldsymbol{\cos\alpha}}{\boldsymbol{\cos^2(\beta - \alpha)}} \boldsymbol{- \cos\beta} \right) \cdot \frac{\cos\theta}{1 - \cos\theta} = 0 \tag{63}$$

$$\frac{\partial k_e^*}{\partial \theta} = \sin\beta \cdot \frac{\boldsymbol{-\sin\theta}}{\boldsymbol{(1 - \cos\theta)^2}} \cdot \frac{1 - \cos(\beta - \alpha)}{\cos(\beta - \alpha)} = 0 \tag{64}$$

$$\frac{\partial k_e^*}{\partial \alpha} = \sin\beta \cdot \frac{\cos\theta}{1 - \cos\theta} \cdot \frac{\boldsymbol{-\sin(\beta - \alpha)}}{\boldsymbol{\cos^2(\beta - \alpha)}} = 0 \tag{65}$$

The situation, when either $\cos\theta$, or $(1 - \cos(\beta - \alpha))$, or $\sin\beta$, or $\sin(\beta - \alpha)$, corresponds to the circle, i.e. $\mu = 0$, and contradicts Definition 2. In (64) $\sin\theta = 0$ cannot be satisfied, since turning the denominator in (62) to 0. The remaining condition in (63), marked in bold, is modified in relation to (36), (37) and (25):

$$\frac{\cos\alpha}{\cos\beta} - \cos^2(\beta - \alpha) = 0 \tag{66}$$

$$\frac{1 - \mu\tau}{\tau - \mu} = \tau^2 \tag{67}$$

$$(1 - \tau)(\tau^2 + \tau + 1 - \mu\tau) = 0 \tag{68}$$

In (68), the first multiplier equals to 0, when $\tau = 1$. This case corresponds to ellipse, thus, $\mu = 1$ and the denominator in (61) turns to 0. The second multiplier is a quadratic equation without the real roots. All in all, it enables to conclude, that k_e^* is a valid part of the error function, since being nonlinear and monotonic for the defined ranges of values (Sect. 4.1): $\theta \in (0, \frac{\pi}{2})$, $(\beta - \alpha) \in [0, \frac{\pi}{4})$, $\beta \in (0, \frac{\pi}{2})$.

6 Experiments

When evaluating the algorithm in the digital domain, two aspects are important to consider: (a) the computational complexity and (b) the accuracy. Regarding the first aspect, Algorithm 1.1 is linear with a potential for parallel execution (Sect. 5).

The proposed method accumulates the errors from (a) discrete egg-shape sampling, (b) rasterization, (c) SEC, and (d) DT. Irrespective of digital image artefacts, the type of sampling (nonuniform/uniform), as well as the number of its members, affect the deviation of parameter estimates from the groundtruth. So, computing a single triplet of values (Lines 1–3) might not lead to an accurate result. A solution to this problem is to take various combinations of $(k,\ r,\ R)$

and select the one, that has a higher similarity to the input shape according to Jaccard index [9]. This process has a benefit of computing distinct triplets in parallel. During rasterization, the x-, y-coordinates of the egg-shape points are rounded to the nearest natural number. Then, the corresponding maximum error equals half-length of the pixel diagonal (HPD). The error of estimating SEC is bounded by the accuracy of rasterization and sampling. DT result depends on the selected method and metric. The exact Euclidean DT algorithm [2] enables mitigating extra errors caused by distance propagation and image transformation to some canonical form. It bounds the maximum error of measuring the distance on a digital grid to HPD. The total error of estimating k equals $(3 \times HPD + e^k_{sa})$; r - $(2 \times HPD + e^r_{sa})$; R - $(HPD + e^R_{sa})$. Here, e^*_{sa} denotes the sampling error.

For comparison with the state-of-the-art work of Hladůvka et al. [9], the test dataset considers 6272 egg-shapes. They are computed for $R_{gt} = 100$ and μ_{gt} varying from 0.01 to 1 with the step 0.01. Each μ_{gt}-value is mapped to the set of τ_{gt}-values within the range specified in Sect. 4.1 and step 0.01. The test dataset contains uniform and nonuniform samplings with $N = 40$ and $N = 500$ points. The corresponding binary images have the size 512×512. The quality is measured as the difference between the groundtruth and the estimated μ. Table 2 summarizes the percentage of cases, when $|\mu - \mu_{gt}|$ is less than 0.01 and 0.1. The egg-shapes that resemble an oval or have a sharp corner ($\mu > 0.1$ and $\frac{c}{f} < 2$) lead to more accurate results, due to uniqueness of their form. For the proposed method this error is less than or equal to 0.1 in 98.7% and 99.8% of cases for $N = 40$ and $N = 500$ respectively. Almost 37% of the dataset contains nearly circular shapes ($\mu \leq 0.1$ or $\frac{c}{f} \geq 2$). The subtle differences between them are hardly visible to human (Fig. 5) and are challenging for both algorithms. The proposed algorithm rests on the exact solution, whereas [9] approximates the relative correspondence between the egg-shape parameters. As a result, the present work shows better performance in all the observed scenarios.

Table 2. Experimental results.

		40				**500**			
	$\lvert\mu - \mu_{gt}\rvert$	nonuniform	uniform	circular	oval	nonuniform	uniform	circular	oval
our	≤ 0.01	34.6%	42.2%	20.4%	48.9%	51.7%	54.8%	25.8%	69.4%
	≤ 0.1	87.1%	86.7%	67.2%	98.7%	91.3%	91.2%	76.5%	99.8%
[8]	≤ 0.01	30.9%	34.4%	6.1%	48.2%	41.6%	48.5%	7.8%	66.9%
	≤ 0.1	74.5%	73.8%	35.2%	97%	67.4%	79.2%	37.3%	94.5%



(a) $\frac{c}{f} = 1.06$ (b) $\frac{c}{f} = 1.17$ (c) $\frac{c}{f} = 1.92$ (d) $\frac{c}{f} = 2.3$

Fig. 5. The egg-shapes (grey area) with two foci (black dots) and SEC (dotted) corresponding to $\mu = 0.29$ and various $\frac{c}{f}$

7 Conclusion and Outlook

The paper contributes to the state-of-the-art in several ways: (a) the egg-shape study relatively to its SEC, (b) the discovery of the geometric properties that explain the foci locations through the weight μ, (c) the derivation of the egg-shape parameters through SEC and largest inscribed circle, (d) the introduction of the linear (with a potential parallel execution) algorithm to find the egg-shape parameters given a binary image. The experiments on synthetic data revealed the ability of the method to perform reliably even in challenging scenarios, when the shape is nearly circular. The primary direction of the future work is to adapt algorithm for real world applications in the presence of noise and occlusions. The second focus is on generalization of the established geometric properties for more than two foci and higher dimensions. The third line of research approaches the 3D case, in particular, its projections onto 2D from different viewpoints.

Disclosure of Interests. The authors have no competing interests.

References

1. Chrystal, G.: On the problem to construct the minimum circle enclosing N given points in the plane. Proc. Edinb. Math. Soc. **3**, 30–33 (1884)
2. Ciesielski, K.C., Chen, X., Udupa, J.K., Grevera, G.J.: Linear time algorithms for exact distance transform. J. Math. Imaging Vision **39**(3), 193–209 (2011)
3. da Fontoura Costa, L., Cesar, Jr., R.M.: Shape Analysis and Classification: Theory and Practice. CRC Press LLC, Boca Raton, 1st edn. (2000)
4. Gabdulkhakova, A.: From circles to generalized conics: Enriching the properties of 2D shape representation and description. Tech. Rep. PRIP-TR-156, Pattern Recognition and Image Processing Group, Technische Universität Wien (2022)
5. Gellert, W., Hellwich, M., Kästner, H., Küstner, H.: The VNR Concise Encyclopedia of Mathematics, 2nd edn. Springer, New York, New York (2012)
6. Glaeser, G., Stachel, H., Odehnal, B.: The Universe of Conics: From the Ancient Greeks to 21st Century Developments, 2nd edn. Springer, Berlin, Heidelberg (2016)
7. Gonzalez, R., Woods, R.: Digital Image Processing, 4th edn. Pearson, New York (2017)
8. Groß, C., Strempel, T.K.: On generalizations of conics and on a generalization of the Fermat-Torricelli problem. Am. Math. Mon. **105**(8), 732–743 (1998)

9. Hladůvka, J., Kropatsch, W.G.: Fitting egg-shapes to discretized object boundaries. In: Brunetti, S., Frosini, A., Rinaldi, S. (eds.) Discrete Geometry and Mathematical Morphology (DGMM 2024), LNCS, vol. 14605, pp. 107–119. Springer, Cham (2024). https://doi.org/10.1007/978-3-031-57793-2_9
10. Maxwell, J.C.: The Scientific Letters and Papers of James Clerk Maxwell: Volume 1, 1846-1862. Cambridge University Press, Cambridge, 1st edn. (1990)
11. Melzak, Z.A., Forsyth, J.S.: Polyconics. I. Polyellipses and optimization. Q. Appl. Math. **35**(2), 239–255 (1977)
12. Nie, J., Parrilo, P.A., Sturmfels, B.: Semidefinite Representation of the k-Ellipse. In: Algorithms in Algebraic Geometry. The IMA Volumes in Mathematics and its Applications, vol. 146, pp. 117–132. Springer, New York (2008). https://doi.org/10.1007/978-0-387-75155-9_7
13. Sekino, J.: n-ellipses and the minimum distance sum problem. Am. Math. Mon. **106**(3), 193–202 (1999)
14. Welzl, E.: Smallest enclosing disks (balls and ellipsoids). In: Maurer, H. (ed.) New Results and New Trends in Computer Science. LNCS, vol. 555, pp. 359–370. Springer, Heidelberg (1991). https://doi.org/10.1007/BFb0038202
15. Williamson, B.: The properties of the Cartesian oval treated geometrically. Hermathena **2**(4), 509–518 (1876)